

Applying green $\text{Ca}_2\text{Al}_3\text{O}_6\text{F}:\text{Eu}^{2+}$ oxyfluoride phosphorus on white emitting diodes

Van Liem Bui¹, Dieu An Nguyen Thi²

¹Faculty of Fundamental Science, Industrial University of Ho Chi Minh City, Ho Chi Minh City, Vietnam

²Faculty of Electrical Engineering Technology, Industrial University of Ho Chi Minh City, Ho Chi Minh City, Vietnam

Article Info

Article history:

Received Nov 30, 2021

Revised Jun 4, 2022

Accepted Jun 24, 2022

Keywords:

$\text{Ca}_2\text{Al}_3\text{O}_6\text{F}:\text{Eu}^{2+}$

Color uniformity

Luminous flux

Mie-scattering theory

White lighting-emitting diodes

ABSTRACT

$\text{Ca}_2\text{Al}_3\text{O}_6\text{F}:\text{Eu}^{2+}$, a new green-emitting and its photoluminescence (PL) characteristics for white lighting-emitting diodes (w-LEDs), have been analyzed and generated. This phosphorus displays a strong absorption range between ultraviolet (UV) and blue region, along with a wide green emission range of 502 nm. The procedure for concentration quenching and Eu^{2+} luminous longevity has been investigated using $\text{Ca}_2\text{Al}_3\text{O}_6\text{F}:\text{Eu}^{2+}$ phosphors. Key characteristics for manufacturing w-LED lamps, such as photoluminescence based on temperature, microstructure, morphology, CIE value and quantum efficiency, were also investigated in $\text{Ca}_2\text{Al}_3\text{O}_6\text{F}:\text{Eu}^{2+}$. The findings show that $\text{Ca}_2\text{Al}_3\text{O}_6\text{F}:\text{Eu}^{2+}$, is a suitable option for almost UV-excited w-LEDs as a green component.

This is an open access article under the [CC BY-SA](https://creativecommons.org/licenses/by-sa/4.0/) license.



Corresponding Author:

Dieu An Nguyen Thi

Faculty of Electrical Engineering Technology, Industrial University of Ho Chi Minh City

No. 12 Nguyen Van Bao Street, Ho Chi Minh City, Vietnam

Email: nguyenthidieuan@iuh.edu.vn

1. INTRODUCTION

Contemporary phosphorus conversion of white lighting-emitting diodes (w-LEDs), due to their major benefits over standard fluorescent lamps and incandescent bulbs, has received significant interest, such as extended operating duration, substantial energy efficacy, low heat emission, and exempt from mercury. The majority of merchandising w-LEDs are made up of a mix including blue emitting LEDs as well as yellow phosphorus $\text{Y}_3\text{Al}_5\text{O}_{12}:\text{Ce}^{3+}$ (YAG:Ce) [1]-[3]. Due to limited amount of red emitting element, these w-LEDs is poor in term of color rendering indice (CRI). w-LEDs, produced with a near ultraviolet (n-UV) LED of 350-420 nm, have therefore been examined to enhance the CRI values by means of three main colour outputs blended from red, green and blue color phosphorus [4]-[6]. The luminous qualities of the phosphor employed substantially influence the final presentation of w-LED-based units. Studies into novel phosphors excited by n-UV light have swiftly grown and turned out to be among of the most popular areas for research in the phosphorus field. Since the Eu^{2+} 4f-5d transition is susceptible to crystal with covalency, Eu^{2+} -doped phosphorus typically exhibits a better spectrum absorption of 250-400 nm, equal to ultraviolet as well as near-ultraviolet chip of lighting-emitting diode (LED) [7]-[9]. Moreover, large emitting bands are shown, ranging between blue color and red color bands. In order to solve greater efficiency concerns, improved colour rendering in company with enhanced chemical and heat consistency, several attempts are under way to create novel w-LED phosphorous products including Eu^{2+} silicates, aluminates, nitrides/oxy-nitrides featuring compounds incorporating halogen [10]-[13].

Currently, oxides with halogen-containing rare earth ions are promising as w-LED phosphorus, which, because of the introduction of hosts halogen particles (F, Cl, and Br), has adjustable luminous

characteristics. In the current quest for novel compounds with fascinating luminescence characteristics with the arrival of rare-earth particles, oxyhalides, notably oxyfluorides, have been a revived target of experimental production [14], [15]. One recent example of oxyfluoride-based phosphors was $\text{Sr}_3\text{AlO}_4\text{F}:\text{Ce}^{3+}$ focused, with efficient blue-green Ce^{3+} in n-UV excitation, as well as developing several modified $\text{Sr}_3\text{AlO}_4\text{F}$ -based phosphors. The new host $\text{Sr}_3\text{AlO}_4\text{F}$'s structural composition is obtained by replacing F with O_2 , which is balanced through replacing Al^{3+} with Si^{4+} in Sr_3SiO_5 . A recent study done by Im *et al.* revealed that it can be solved between $\text{Sr}_3\text{AlO}_4\text{F}$ and Sr_3SiO_5 , which are almost isostructural, and that certain good optimal luminescence characteristics have been documented also [16]. We thus note that $\text{Ca}_2\text{Al}_3\text{O}_6\text{F}$ is a noteworthy phosphorus host with a tetragonal melilite-type configuration. The novel molecule with the chemical formula $\text{Ca}_2\text{Al}_3\text{O}_6\text{F}$ in this arrangement can be produced if the chemical replacement of F for O_2 , which is made up by Al^{3+} for Si^{4+} , is likewise efficient. The early structural data of $\text{Ca}_2\text{Al}_3\text{O}_6\text{F}$, entirely different than the $\text{Ca}_2\text{Al}_2\text{SiO}_7$ stage, may be attained on the query premise in the joint committee on powder diffraction standards (JCPDS) dataset. Nevertheless, when we check for novel phosphorus compositions of renowned phosphorus hosts, it obviously offers a successful method. $\text{Ca}_2\text{Al}_3\text{O}_6\text{F}$ phases [17]-[19]. Here, an effective host for phosphorus materials for the $\text{Ca}_2\text{Al}_3\text{O}_6\text{F}$ is suggested. We notice and note down all the features of the compounds Eu^{2+} doped $\text{Ca}_2\text{Al}_3\text{O}_6\text{F}$, which could be w-LEDs stimulated with n-UV chip phosphorous, such as the synthesis, initial structural characterization and luminescence characteristic.

2. RESEARCH METHOD

2.1. Ingredients and production

A solid-state reaction, which is in high heat, approach produced the host chemical $\text{Ca}_2\text{Al}_3\text{O}_6\text{F}$ and the $\text{Ca}_{2-x}\text{Al}_3\text{O}_6\text{F}:\text{xEu}^{2+}$ phosphors. Initial ingredients include Aldrich 99.9% of CaCO_3 , Al_2O_3 , CaF_2 and Eu_2O_3 (Aldrich, 99.995%). All initial ingredients was combined and ground in a standard process, according to the stated stoichiometric ratio. To counteract the F source deficiency at extreme temperatures, a little excess of CaF_2 (5 wt% above stoichiometry) is needed. After the combination were completely ground in a mortar of agate, they were put in an aluminum crucible and were burned at 1250 °C ($\text{N}_2\text{-H}_2$ 1/4-95: 5) for 4 hours in a reducing environment. Afterwards, the combination was chilled to normal temperature in a furnace before being powdered for later [20], [21]. The final phosphor product is applied on a w-LED device used for this study, whose model can be seen in Figure 1.

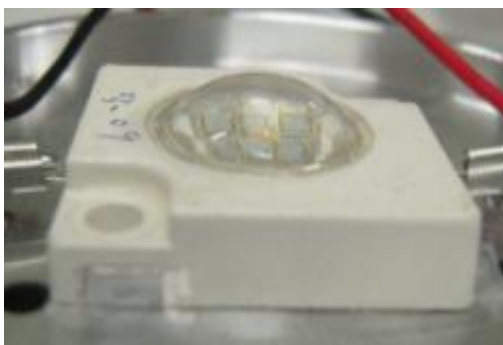


Figure 1. Photograph of w-LEDs

2.2. Reflection and Eu^{2+} doped $\text{Ca}_2\text{Al}_3\text{O}_6\text{F}$ photoluminescence spectrum

As shown in (1) is an acceptable match for the emission peak and the excitation edge data according to Van Uitert report 30 on Eu^{2+} in an appropriate matrix. The potential crystallographic site in $\text{Ca}_2\text{Al}_3\text{O}_6\text{F}$ replaced by Eu^{2+} may be examined hypothetically on the basis of this equation. This equation is shown as (3) [22], [23].

$$E = Q \left[1 - \left(\frac{V}{4} \right)^{\frac{1}{V}} 10^{-\frac{nE_a r}{80}} \right] \quad (1)$$

In the first equation, E represents the energy location of the rare terrestrial particle's d-band border (cm^{-1}), Q represents the energy location of the free particle's lower d-belt edge ($34\,000\ \text{cm}^{-1}$ for Eu^{2+}) while V is the "active" cation value, in this case $V=2$ for Eu^{2+} . E_a denotes the anion-forming ions electrical affinity,

which is variable in distinct anion complexes as Eu^{2+} is involved to other coordinate numbers. Here, E_a is calculated roughly as 2.5, as seen in previous designs of the melilite; n denotes the "active" cation's immediate shell quantity of anions while r is the host cation radius (Ca^{2+}) substituted by the "active" cation (Eu^{2+}).

According to Blasse, the crucial spacing (R_c) between two equal centers is measured as the area at which the conversion of energy is equivalent to the radiative energy emissions likelihood of Eu^{2+} [24]. The calculation of the R_c value is based on 32 as shown in (2),

$$R_c \approx 2 \left(\frac{3V}{4\pi x_c N} \right)^{\frac{1}{3}} \quad (2)$$

where R_c is the median distance from the closest Eu^{2+} particles at x_c . Utilizing $V=1819.26$ Å, $N=12$, as well as $x_c=0.05$, the crucial conversion range of Eu^{2+} in $\text{Ca}_2\text{Al}_3\text{O}_6\text{F}$ is 17.96 Å. Because interaction between Eu^{2+} ions is only dominant over small ranges, the contact mechanism does not play a role in conversion of energy among Eu^{2+} particles in $\text{Ca}_2\text{Al}_3\text{O}_6\text{F}$ phosphorous (5 Å typical crucial ranges). Consequently, only through electric multipolar connections would the energy transfer take place in the current situation. Three multipole-multipole interactions are based on the theory of Dexter: dipole-dipole, dipole-quadrupole, and quadrupole-quadrupole, accordingly. We can calculate the emission intensity (I) of the multiple interactions by adjusting the emitting density from the emitting level featuring the multipolar contact [25], as shown in (3).

$$\frac{I}{x} = K \left[1 + \beta(x)^{\frac{\theta}{3}} \right]^{-1} \quad (3)$$

In which I denotes the emitting density x is the activator particle concentration, the constant of K and is β the multipole-multipole role interactions, the values of 6 (dipole-dipole), 8 (dipole-quadrupole) or 10 (quadrupole-quadrupole), respectively. The phosphorus film of real multi-chip white LED (MCW-LEDs) is replicated by flat silicone films, according to the LightTools 9.0 program and Monte Carlo technique. This simulation works across two major stages: the MCW-LED configuration models and the optic characteristics should be defined as well as constructed. $\text{Ca}_2\text{Al}_3\text{O}_6\text{F}:\text{Eu}^{2+}$ concentration variation thus regulates the phosphor compounding optical effects effectively. We must make some contrast to assess the impact on MCW-LED lamps emission using $\text{YAG}:\text{Ce}^{3+}$ and $\text{Ca}_2\text{Al}_3\text{O}_6\text{F}:\text{Eu}^{2+}$ phosphorus compositions. The two types of compounds have to be clarified with median CCTs range between 3,000 K; 4,000 K; and 5,000 K two-layer distant phosphorus. A thorough description of the conformal phosphorus compounder MCW-LED lamps with a 8500 K median CCT is given in Figure 1 MCW-LEDs modeling of whose components do not contain $\text{Ca}_2\text{Al}_3\text{O}_6\text{F}:\text{Eu}^{2+}$ is also recommended. The reflector measures are 8, 2.07 and 9.85 (measured in mm) in bottom length, height and top surface, correspondingly. The composite compound of conformal phosphorus wraps nine chips with a thickness of each is 0.08 mm. Every LED chip is connected with the reflector chamber whose base region is 1.14 mm² and altitude is 0.15 mm. The illuminating beam is 1.16 W for every blue chip, whereas the maximum wavelength is 453 nm.

3. RESULTS AND ANALYSIS

The shift in green $\text{Ca}_2\text{Al}_3\text{O}_6\text{F}:\text{Eu}^{2+}$ concentration and yellow $\text{YAG}:\text{Ce}^{3+}$ phosphorus concentration in Figure 2, is the inverse. Such modification has these purposes: the first is for the preservation of average CCT, the second is for the absorption and dispersion of two phosphorus layers. This eventually impacts the hue standard and the effectiveness of the w-LEDs illuminating beam. w-LEDs colour standard may therefore be determined by selecting $\text{Ca}_2\text{Al}_3\text{O}_6\text{F}:\text{Eu}^{2+}$. The $\text{YAG}:\text{Ce}^{3+}$ concentration refused the preservation of the average CCTs while the $\text{Ca}_2\text{Al}_3\text{O}_6\text{F}:\text{Eu}^{2+}$ went from 2% to 20% wt. The same applies to w-LEDs with colour temperatures ranging between 5,600-8,500 K.

The influence of the green $\text{Ca}_2\text{Al}_3\text{O}_6\text{F}:\text{Eu}^{2+}$ phosphorus concentration on the transmitting bands of color of w-LEDs can be seen clearly in Figure 3. It is feasible to make a selection based on the criteria established by the producer. w-LEDs with excellent grade colors might luminous flux w to a small extent. The spectral area like Figure 3 is a synthesis of white light. The spectrum of this figure is 5,000 K. The intensity trend with $\text{Ca}_2\text{Al}_3\text{O}_6\text{F}:\text{Eu}^{2+}$ concentration obviously increases two light spectrum regions 420-480 nm and 500-640 nm. The rise in the two-range bands of color shows a growth of the luminous productivity. In addition, w-LEDs have improved blue-light dispersion, implying that scattering in the phosphorous layer and w-LEDs expand, leading to color homogeneity. This is a significant result for $\text{Ca}_2\text{Al}_3\text{O}_6\text{F}:\text{Eu}^{2+}$ applications. In details, the high-temperature remote phosphorus arrangement's color homogeneity is

challenging to regulate. This investigation verified that the color quality of WLEDs may be improved by $\text{Ca}_2\text{Al}_3\text{O}_6\text{F}:\text{Eu}^{2+}$, including the 5,600 K less high and the 8,500 K high of hue heat.

This article illustrates the illuminating flux efficacy emitted from such distant phosphorus layer. The results in Figure 4 in particular indicated that the emitted luminous flux grew dramatically when the $\text{Ca}_2\text{Al}_3\text{O}_6\text{F}:\text{Eu}^{2+}$ concentration rised 2%-20% wt. The hue deviation at all three average CCTs has been considerably decreased according to the findings of Figure 5, using phosphorus $\text{Ca}_2\text{Al}_3\text{O}_6\text{F}:\text{Eu}^{2+}$. The red phosphor absorption clarifies this. The blue phosphoric ions in the $\text{Ca}_2\text{Al}_3\text{O}_6\text{F}:\text{Eu}^{2+}$ phosphorous receive the blue light from an LED chip, converting it to green light. $\text{Ca}_2\text{Al}_3\text{O}_6\text{F}:\text{Eu}^{2+}$ particles receive the LED chip yellow and blue light. Yet, the LED chip blue light absorption is more severe owing to the material's absorption characteristics than these two absorbs. Thus, using $\text{Ca}_2\text{Al}_3\text{O}_6\text{F}:\text{Eu}^{2+}$, the green light concentration in w-LEDs as well as the color consistencies index improved. Color uniformity among modern w-LED lamp parameters is among the major criteria. The cost of w-LED light increases as the color homogeneity indice rises. $\text{Ca}_2\text{Al}_3\text{O}_6\text{F}:\text{Eu}^{2+}$ is cheap which is an advantage. This allows the extensive usage of $\text{Ca}_2\text{Al}_3\text{O}_6\text{F}:\text{Eu}^{2+}$.

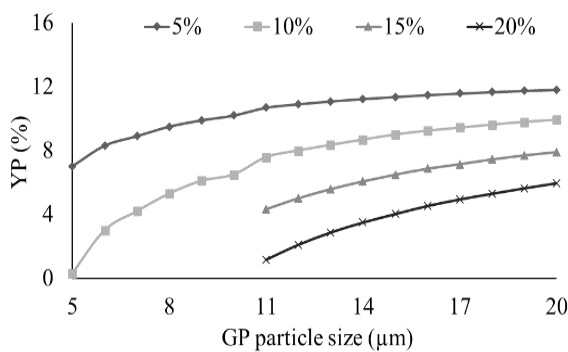


Figure 2. The modification of phosphor concentration to keep the median CCT value

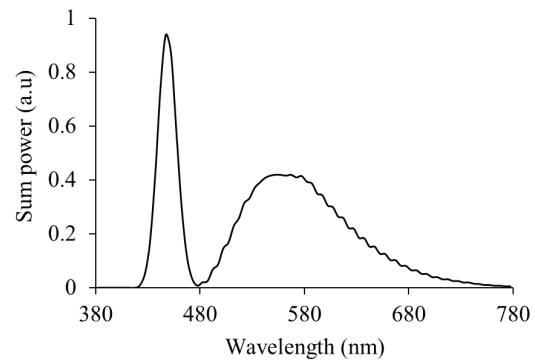


Figure 3. $\text{Ca}_2\text{Al}_3\text{O}_6\text{F}:\text{Eu}^{2+}$ concentration functions as the 5,000 K w-LEDs emission spectrum

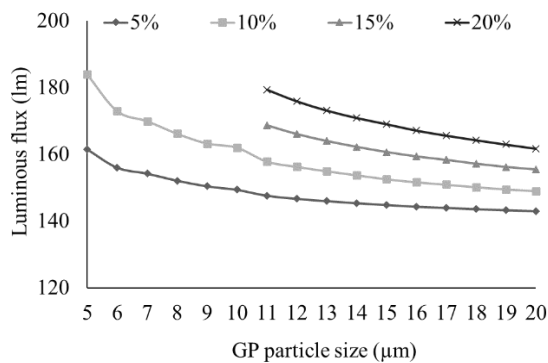


Figure 4. $\text{Ca}_2\text{Al}_3\text{O}_6\text{F}:\text{Eu}^{2+}$ concentration functions the w-LEDs luminance flux

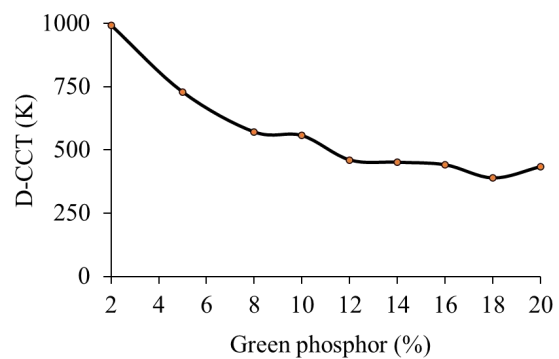


Figure 5. The hue deviation of w-LEDs as a function of $\text{Ca}_2\text{Al}_3\text{O}_6\text{F}:\text{Eu}^{2+}$ concentration

In analyzing the quality of colors of w-LEDs, color uniformity is simply one criterion. With just a elevated hue uniformity rating, acceptable color quality can indeed be claimed. Latest research thus gives a colour rendering indice and a colour quality scale. As a light illumines the color rendering indice, item's genuine color is evaluated. This color imbalance is due to the excessive green light ranging from blue, yellow and green. w-LED colour quality suffers as a result, and color dependability declined. The findings in Figure 6 suggest a small drop in CRI when the distant $\text{Ca}_2\text{Al}_3\text{O}_6\text{F}:\text{Eu}^{2+}$ phosphorus layer is present. These are allowed, though, because CRI is just a color quality scale (CQS) vulnerability. The CQS is more significant and difficult to attain when comparing between CRI and CQS. This is an index of three elements: first, the color rendering index, second is the CQS and third is the preference of the viewer. For those prominent elements, CQS is virtually a genuine total colour quality measure. Figure 7 demonstrates the improvement of CQS in the presence of the remote phosphorus $\text{Ca}_2\text{Al}_3\text{O}_6\text{F}:\text{Eu}^{2+}$ layer. Furthermore, with a concentration of

$\text{Ca}_2\text{Al}_3\text{O}_6\text{F}:\text{Eu}^{2+}$ less than 10% wt, CQS does not vary considerably when the level of the phosphor increases. CRI and CQS are lowered considerably because of the severe color loss when green is dominant with a $\text{Ca}_2\text{Al}_3\text{O}_6\text{F}:\text{Eu}^{2+}$ concentration over 10% wt. Applying green phosphorus $\text{Ca}_2\text{Al}_3\text{O}_6\text{F}:\text{Eu}^{2+}$ thus requires a proper concentration selection.

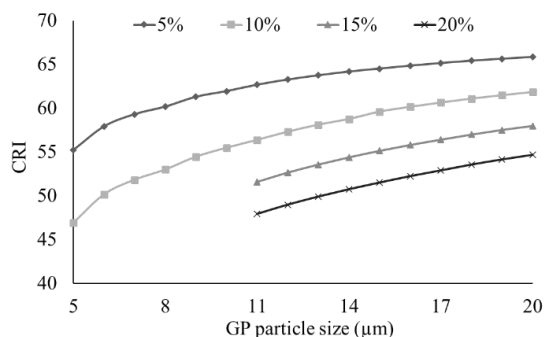


Figure 6. The color rendering index of w-LEDs as a function of $\text{Ca}_2\text{Al}_3\text{O}_6\text{F}:\text{Eu}^{2+}$ concentration

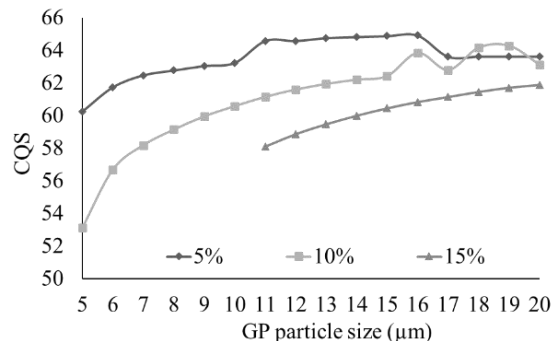


Figure 7. $\text{Ca}_2\text{Al}_3\text{O}_6\text{F}:\text{Eu}^{2+}$ concentration functions as the w-LEDs hue standard $\text{Ca}_2\text{Al}_3\text{O}_6\text{F}:\text{Eu}^{2+}$ d scale

4. CONCLUSION

This article depicts the influence of the green $\text{Ca}_2\text{Al}_3\text{O}_6\text{F}:\text{Eu}^{2+}$ double-level phosphor structure on optical characteristics. The study shows that $\text{Ca}_2\text{Al}_3\text{O}_6\text{F}:\text{Eu}^{2+}$ is an adequate solution to enhance hue homogeneity based on Monte Carlo computer simulations. It relates not just to w-LEDs of 5,000 K, but also to ones with a color temperature higher than 8,500 K. Therefore, the results of this study have met the goal of enhancing colour, light, and the phosphorus remote configuration is extremely difficult. But CRI and CQS have a slight disadvantage. When the $\text{Ca}_2\text{Al}_3\text{O}_6\text{F}:\text{Eu}^{2+}$ concentration is greatly raised, the CRI decreases substantially with the CQS. The right concentration must thus be chosen based on the manufacturer's aims. In terms of increased hue homogeneity and illuminating WLEDs, this study has supplied a wealth of useful data which will be helpful in future research.




REFERENCES

- [1] H. Lee, S. Kim, J. Heo, and W. J. Chung, "Phosphor-in-glass with Nd-doped glass for a white LED with a wide color gamut," *Optics Letters*, vol. 43, no. 4, p. 627, Feb. 2018, doi: 10.1364/OL.43.000627.
- [2] Y. Park, K. H. Li, W. Y. Fu, Y. F. Cheung, and H. W. Choi, "Packaging of InGaN stripe-shaped light-emitting diodes," *Applied Optics*, vol. 57, no. 10, p. 2452, Apr. 2018, doi: 10.1364/AO.57.002452.
- [3] W. Gao, K. Ding, G. He, and P. Zhong, "Color temperature tunable phosphor-coated white LEDs with excellent photometric and colorimetric performances," *Applied Optics*, vol. 57, no. 31, p. 9322, Nov. 2018, doi: 10.1364/AO.57.009322.
- [4] Y. Tang, Z. Li, G. Liang, Z. Li, J. Li, and B. Yu, "Enhancement of luminous efficacy for LED lamps by introducing polyacrylonitrile electrospinning nanofiber film," *Optics Express*, vol. 26, no. 21, p. 27716, Oct. 2018, doi: 10.1364/oe.26.027716.
- [5] J.-H. Kim, B.-Y. Kim, and H. Yang, "Synthesis of Mn-doped CuGaS₂ quantum dots and their application as single downconverters for high-color rendering solid-state lighting devices," *Optical Materials Express*, vol. 8, no. 2, p. 221, Feb. 2018, doi: 10.1364/OME.8.000221.
- [6] T. Han *et al.*, "Spectral broadening of a single Ce³⁺-doped garnet by chemical unit cosubstitution for near ultraviolet LED," *Optical Materials Express*, vol. 8, no. 12, p. 3761, Dec. 2018, doi: 10.1364/ome.8.003761.
- [7] Z. Li, Y. Tang, J. Li, X. Ding, C. Yan, and B. Yu, "Effect of flip-chip height on the optical performance of conformal white-light-emitting diodes," *Optics Letters*, vol. 43, no. 5, p. 1015, Mar. 2018, doi: 10.1364/OL.43.001015.
- [8] Z. Song, T. Guo, X. Fu, and X. Hu, "Residual vibration control based on a global search method in a high-speed white light scanning interferometer," *Applied Optics*, vol. 57, no. 13, p. 3415, 2018, doi: 10.1364/ao.57.003415.
- [9] S.-R. Chung, C.-B. Siao, and K.-W. Wang, "Full color display fabricated by CdSe bi-color quantum dots-based white light-emitting diodes," *Optical Materials Express*, vol. 8, no. 9, p. 2677, Sep. 2018, doi: 10.1364/OME.8.002677.
- [10] R. Melikov *et al.*, "Eco-friendly Silk-hydrogel Lenses for LEDs," in *Advanced Photonics 2018 (BGPP, IPR, NP, NOMA, Sensors, Networks, SPPCom, SOF)*, 2018, vol. Part F107-, p. NoW4D.4, doi: 10.1364/NOMA.2018.NoW4D.4.
- [11] J. Sun, H. Hao, W. Xu, Y. Song, Y. Wang, and X. Zhang, "Manipulation of microstructures and the stability of white emissions in NaLuF₄:Yb³⁺, Ho³⁺, Tm³⁺ upconversion crystals," *Optical Materials Express*, vol. 8, no. 4, p. 1043, Apr. 2018, doi: 10.1364/ome.8.001043.
- [12] V. Bahrami-Yekta and T. Tiedje, "Limiting efficiency of indoor silicon photovoltaic devices," *Optics Express*, vol. 26, no. 22, p. 28238, Oct. 2018, doi: 10.1364/OE.26.028238.
- [13] B. Li *et al.*, "High-efficiency cubic-phased blue-emitting Ba₃Lu₂B₆O₁₅:Ce³⁺ phosphors for ultraviolet-excited white-light-emitting diodes," *Optics Letters*, vol. 43, no. 20, p. 5138, Oct. 2018, doi: 10.1364/ol.43.005138.
- [14] S. Cincotta, C. He, A. Neild, and J. Armstrong, "High angular resolution visible light positioning using a quadrant photodiode angular diversity aperture receiver (QADA)," *Optics Express*, vol. 26, no. 7, p. 9230, Apr. 2018, doi: 10.1364/OE.26.009230.




- [15] Q. Hu, X. Jin, and Z. Xu, "Compensation of sampling frequency offset with digital interpolation for OFDM-based visible light communication systems," *Journal of Lightwave Technology*, vol. 36, no. 23, pp. 5488–5497, Dec. 2018, doi: 10.1109/JLT.2018.2876042.
- [16] A. I. Alhassan *et al.*, "Development of high performance green c-plane III-nitride light-emitting diodes," *Optics Express*, vol. 26, no. 5, p. 5591, Mar. 2018, doi: 10.1364/OE.26.005591.
- [17] J. Cheng *et al.*, "Luminescence and energy transfer properties of color-tunable Sr 4 La(PO 4) 3 O: Ce 3+ , Tb 3+ , Mn 2+ phosphors for WLEDs," *Optical Materials Express*, vol. 8, no. 7, p. 1850, Jul. 2018, doi: 10.1364/OME.8.001850.
- [18] J.-S. Li, Y. Tang, Z.-T. Li, L.-S. Rao, X.-R. Ding, and B.-H. Yu, "High efficiency solid-liquid hybrid-state quantum dot light-emitting diodes," *Photonics Research*, vol. 6, no. 12, p. 1107, Dec. 2018, doi: 10.1364/PRJ.6.001107.
- [19] Y. Peng *et al.*, "Flexible fabrication of a patterned red phosphor layer on a YAG:Ce 3+ phosphor-in-glass for high-power WLEDs," *Optical Materials Express*, vol. 8, no. 3, p. 605, Mar. 2018, doi: 10.1364/ome.8.000605.
- [20] K. Werfli *et al.*, "Experimental demonstration of high-speed 4 × 4 imaging multi-CAP MIMO visible light communications," *Journal of Lightwave Technology*, vol. 36, no. 10, pp. 1944–1951, May 2018, doi: 10.1109/JLT.2018.2796503.
- [21] M. Talone and G. Zibordi, "Spatial uniformity of the spectral radiance by white LED-based flat-fields," *OSA Continuum*, vol. 3, no. 9, p. 2501, Sep. 2020, doi: 10.1364/osac.394805.
- [22] W. Zhong, J. Liu, D. Hua, S. Guo, K. Yan, and C. Zhang, "White LED light source radar system for multi-wavelength remote sensing measurement of atmospheric aerosols," *Applied Optics*, vol. 58, no. 31, p. 8542, Nov. 2019, doi: 10.1364/AO.58.008542.
- [23] S. Feng and J. Wu, "Color lensless in-line holographic microscope with sunlight illumination for weakly-scattered amplitude objects," *OSA Continuum*, vol. 2, no. 1, p. 9, Jan. 2019, doi: 10.1364/OSAC.2.000009.
- [24] J. O. Kim, H. S. Jo, and U. C. Ryu, "Improving CRI and scotopic-to-photopic ratio simultaneously by spectral combinations of cct-tunable led lighting composed of multi-chip leds," *Current Optics and Photonics*, vol. 4, no. 3, pp. 247–252, 2020, doi: 10.3807/COPP.2020.4.3.247.
- [25] Y. Zhou *et al.*, "Comparison of nonlinear equalizers for high-speed visible light communication utilizing silicon substrate phosphorescent white LED," *Optics Express*, vol. 28, no. 2, p. 2302, Jan. 2020, doi: 10.1364/oe.383775.

BIOGRAPHIES OF AUTHORS



Van Liem Bui    received a Bachelor of Mathematical Analysis and master's in mathematical Optimization, Ho Chi Minh City University of Natural Sciences, Viet Nam. Currently, He is a lecturer at the Faculty of Fundamental Science, Industrial University of Ho Chi Minh City, Viet Nam. His research interests are Mathematical Physics. He can be contacted at email: buivanliem@iuh.edu.vn.



Dieu An Nguyen Thi    received a master of Electrical Engineering, HCMC University of Technology and Education, Viet Nam. Currently, she is a lecturer at the Faculty of Electrical Engineering Technology, Industrial University of Ho Chi Minh City, Viet Nam. Her research interests are Theoretical Physics and Mathematical Physics. She can be contacted at email: nguyenthidieuan@iuh.edu.vn.